CACR-96-09

GROUPS OF BREAKING WAVES: EXPERIMENTS

J. Veeramony [1], and I.A. Svendsen,[2] Member, ASCE

Abstract

Experiments were conducted with periodic wave groups incident on a plane beach with a slope of 1:35.05. The wave groups were composed of a series of cnoidal waves with varying wave heights. Emphasis was on obtaining a number of measurements inside the surf-zone. The analysis of the data shows that the location of the start of breaking of the individual waves in a group is affected by the groupiness of the waves. The H/h ratio at breaking was seen to have a wider variation for the individual waves in the group than for monochromatic waves. In all cases, some groupiness was conserved inside the surf-zone, but in some cases it was reversed in the sense that the higher waves in the group before breaking became the smallest after and vice versa. It was also found that even inside the surf-zone, all non-linear interactions result in energy at frequencies that are multiples of the group frequency, although, as expected, the energy is more evenly distributed between the different frequencies. The long wave motion is forced at the group frequency and can be resolved into two components, an incident forced wave and a free standing wave. The standing wave is generated because the free outgoing long wave is reflected at the wavemaker, where there was no absorption of waves. The amplitude of the incident forced wave varies along the tank, whereas the standing wave is shown largely to agree with a linear representation of a free standing wave system.

1 Introduction.

The group structure of waves has been commonly recognized as a primary driving mechanism for the generation of long waves in the offshore region (Longuet-Higgins & Stewart 1962) as well as in the nearshore region (e.g., Symonds et al. 1982, Schäffer & Svendsen 1988, Schäffer 1990). Symonds et al. assumed the forcing of long waves was caused by the time variation of the break point due to the groupiness of the incident wave field and a fixed wave height to water depth ratio in the surf-zone. Schäffer & Svendsen (1988) assumed a fixed break point, thereby preserving the group structure in the surf-zone, and found that, inside the surf-zone, the group structure also caused generation of long waves. Schäffer (1990) combined the above two models, allowing for the variation of groupiness inside the surf-zone and concluded that the mechanism for long wave generation is a combination of the above two models.

List (1991) analyzed field data and found that a substantial level of groupiness survived the breaking process. Laboratory experiments have also been conducted with wave groups formed by two waves with slightly different frequencies by Kostense (1984). Recently, Watson et al. (1994) conducted experiments with wave groups composed of solitary waves of different heights to analyze the generation of low-frequency waves.

Apart from these examples, however, laboratory data for the behavior of wave groups inside the surf-zone is virtually non-existent. The present paper describes an experimental investigation of wave groups with data taken from a large number of locations inside the surf-zone to improve the understanding of the phenomena in that region.

It was found that the breaking of individual waves in the group is different from that of monochromatic waves. The ratio of the wave height to the water depth had a wider variation in the case of wave groups and the largest wave did not necessarily break at the largest depth. The

[1]Graduate Student, Center for Applied Coastal Research, University of Delaware, Newark, DE 19716, USA. Fax: (302) 831-1228

[2]Professor, Center for Applied Coastal Research, University of Delaware, Newark, DE 19716, USA.

group structure inside the surf-zone was found to be a little more complicated than expected. In some cases, partial or full reversal of groupiness was observed immediately after breaking and in other cases the groupiness was changed in a more subtle way. However, some groupiness was transmitted into the surf-zone in all the experiments.

The long wave motion was found to be composed of an incoming bound wave and a free standing wave composed of the free outgoing long wave and its reflection from the wavemaker. This is consistent with the results of Kostense (1984) who absorbed the outgoing long waves in his experiments at the wavemaker and therefore found that the long wave system in his experiments consisted of an incoming forced wave and a free outgoing wave. The seiching modes in the wave tank were found to increase considerably the amplitude of the standing wave. The paper will discuss these problems and also analyze the effects which the groupiness has on the breaking charateristics of the incident short waves.

The organization of the paper is as follows. The experimental setup is described in section 2. The method of wave group generation is described in section 3. The experimental procedure and the repeatability of the experiments is discussed in section 4. The analysis of the data is presented in sections 5-6 and the results of the analysis summarized in section 7.

2 Experimental setup.

The experiments were carried out in the wave flume at the Center for Applied Coastal Research at the University of Delaware. The flume is $30\,m$ long, $0.6\,m$ wide and $1.0\,m$ deep. The flume is equipped with a hydraulically driven piston type wavemaker and, in the following, we let $x = 0\,m$ represent the mean position of the wavemaker. As shown in figure 1, a plane beach with slope 1:35 was installed in the flume. It was made of CORIAN©, a smooth and impermeable sandstone-like material and the toe of the beach was located at $x = 11.85\,m$. For all experiments, the water depth at the constant depth section was kept at $0.40\,m$.

To check the accuracy of the beach, the depth along the centerline of the beach was measured at various locations using a point-gage. The average slope was then calculated according to the least-square error method. This slope was found to be 1:35.05. It turns out that the deviation from the expected slope of 1:35 was largest along the centerline of the tank, whereas near the walls, the deviations were negligible. One of the consequences of this is that the shoreline was at $x = 25.93\,m$ at the centerline and at $x = 25.85\,m$ near the wall. Figure 2 shows the deviation of the measured water depths from the depths calculated assuming a slope of 1:35.05. The maximum deviation is found to be less than 1.5%.

3 Wave group generation.

The primary objective was to study the propagation of wave groups in the surf-zone which required a wide surf-zone so that measurements could be obtained from a large number of locations. To get reasonable surf-zone conditions, we needed fairly long waves with large amplitudes, which meant large values of the Ursell number $U = HL^2/h^3$. Under those conditions, wave groups generated in the conventional way, by adding two sinusoidal waves of slightly different frequencies, lead to significant irregularities because of the large spurious second harmonics generated. Since no theoretical solutions exist for the shape of groups of finite amplitude long waves, it was decided to take advantage of the capability of the wavemaker to generate waves of any chosen shape and compose the wave motion as a series of consecutive cnoidal waves with

varying heights.

All experiments were performed with five waves in each group. The wave height of the individual waves at the wavemaker was specified as

$$H_i = H_m(1 + \frac{G}{2}\sin\frac{2\pi i}{n}); \quad i = 1, \ldots, 5 \tag{1}$$

where H_i represents the height of the i^{th} wave in the group, H_m the mean wave height, and $G = \Delta H/H_m$ is the variation of the wave height in the group. The time series for the wavemaker motion for each cnoidal wave in the group was calculated using the method developed by Goring (1978). This method determines the trajectory of a piston wave maker for the generation of permanent form long waves. The five cnoidal waves in the group with the different wave heights have slightly different wave profiles. These profiles were added together to form a continuous time series by patching them at the time when the particle velocity is zero, that is, at the zero-upcrossing for the surface profiles. The result was a signal for the position of the wavemaker which is continuous in time, and has a continuous first derivative in time, but which has a slight discontinuity in the second derivative at the points of zero-upcrossing for the surface profile.

Seven experiments were performed in all, and the parameters for each experiment are given in Table 1. Qualitatively, the results from W02 and W04, which differs only in mean wave height, were found to be similar to that from W01 and also, the results from W03 and W05 were found to be similar to each other, which indicates that the absolute value of the wave height is of minor importance. On the other hand, the results from the experiments W01, W03, W06 and W07 showed that changes in the short wave period and the level of modulation of the wave height gave significant variation in the wave patterns. As will become apparent from the analysis below, the short wave period is so important because this period is linked to the period of the long wave component of the wave motion which interacts with the natural modes of oscillation in the wave tank. In the following, we limit our discussion to the results from the experiments W01, W03, W06 and W07.

4 Procedure and repeatability of experiments.

Due to the variation of the wave height, long waves are generated in the tank. The long wave motion is largely reflected from the beach. The sudden initiation of wave motion in the tank at the start of each experiment will generate disturbances which will be present during the early stages of the experiments. These disturbances are composed of a combination of the natural modes of the oscillation for the tank. Due to friction and interaction with the breaking process, this part of the motion is expected to disappear after a while, after which the long wave motion will be steady. To allow the long waves to reach this steady state where the initial disturbances have died out, each experiment was run for 30 minutes before data collection started.

The measurements consisted of time series for the water surface variation at a large number of locations in the shoaling region as well as in the surf-zone. Only ten gages, mounted on movable carriages, were available for collecting data from the first five experiments (W01-W05) and nine for the other two (W06, W07). Hence, each experiment was repeated a number of times with different gage positions. Henceforth, each such repetition will be called a 'run'. In all runs, a reference gage was placed at a fixed location, in the constant depth section, for the experiment. The reference location was at $x = 4.6\,m$ for experiments W01-W05 and at

$x = 4.0\,m$ for W06 and W07. The other gages were placed at different locations in each of the (identical) runs of each experiment. Data collection and storage for each of these runs took approximately 15 minutes. Repositioning of the wave gages between the runs of each experiment was done without stopping the wave generation.

The sampling was done at 50 Hz for all the experiments. For experiments W01-W05, 6000 samples were obtained at each location, which corresponded to 16 wave groups for W01 and 9 wave groups for W02-W05. For experiments W06 and W07, 16384 samples were collected which corresponded to 40 and 37 wave groups, respectively. Hence it was possible, by ensemble averaging, to establish an averaged sample corresponding to one group. At the reference location, the ensemble averaged wave group from each run was used to verify that the motion in the flume was at a steady state.

As an example, the results for the experiment W06 mentioned previously is shown for the reference position $x = 4.0\,m$ in figure 3(a). At this position the maximum deviation from the mean was negligible , which also confirms that the wave motion in the tank was steady and each group a very close repetition of the previous. Figure 3(b) similarly shows the variation at a point inside the breaking region and figure 3(c) the variation at $x = 23.1\ m$ which is a point well into the surf-zone. Clearly the variability at these points is much larger. In particular, inside the surf-zone this variability is to some extent caused by variations in the horizontal position of the wave rather than by a variation in the surface elevation at a given phase relative to the breaking front.

We also observe from figure 3 that some secondary crests were present at the wave troughs, especially close to wave breaking point. This could be due to at least three different inaccuracies associated with the way the waves are generated. The first reason is that even for ordinary cnoidal waves satisfying the requirement that the Ursell parameter $HL^2/h^3 = O(1)$, the velocity variation over depth is not uniform as imposed by the piston wave maker. Secondly, the waves generated actually have a much larger amplitude than assumed by the cnoidal wave theory, so that second or higher order effects are non-negligible, which is not accounted for in the first order cnoidal signal used for the wavemaker motion. Finally, the wave group is approximated by a series of slightly different cnoidal waves with a wave height variation given by (1) and added together as described in section 3. This is not known to be a permanent form solution to the Boussinesq equations. Hence, even if the individual waves had been generated perfectly correctly, they would probably interact within the groups and hence modify as they propagate down the tank which is likely to result in the generation of higher order (soliton-like) disturbances. For all these reasons, we would expect the wave motion generated to show some content of high frequency irregularities.

5 Data analysis.

In analyzing the data, each wave in the group was considered separately. The start of a wave was defined as the point of zero upcrossing relative to the mean water level.

In order to prevent the higher harmonic disturbances to be counted as waves, a constraint was used in the analysis outside the surf-zone, that the wave period cannot be less than half the mean wave period at the wavemaker.

In two of the experiments, it was observed that, inside the surf-zone, smaller waves were overtaken and captured by the higher waves. In the region just before this occurred, the wave heights of the smaller waves were too small to be separated from the higher harmonics.

However, these waves still had the steep front characteristic of breaking surf-zone waves. Hence, to count these as waves, the wave steepness above a minimum was used as an additional criteria inside the surf-zone.

The wave heights of the individual waves were calculated as the difference between the maximum and minimum surface elevation between successive upcrossing points. With the knowledge that every fifth wave was the same, the variation of the individual waves were found as they propagated towards shore.

6 Discussion of Results.

6.1 Variation of the break point.

One of the important questions is how the groupiness of the waves influences the breaking points and the wave heights at breaking. From a record of the surface elevation taken with the type of wave gage used, it is not possible to determine where the water surface becomes vertical. Therefore, other means were used to identify the location of the breaking point.

No definitive method has been developed for prediction of the breaker point and breaker height, even for regular waves. A review of the variety of methods, which are at present widely used for the prediction of wave heights at breaking, is given in Southgate (1993). All these methods of prediction are based on empirical formulations using available experimental data.

It is known that both the absolute wave height and the wave height to water depth ratio have a maximum at or near the breaking point. The value of both these parameters were analysed and the corresponding break points turned out only to differ marginally. In the following analysis we have used the maximum of the wave height to water depth ratio as definition of the break point, which corresponds to

$$\left(\frac{H}{h}\right)_b \equiv \left(\frac{H}{h}\right)_{max}. \tag{2}$$

The wave heights, phase speed and the wave period obtained from the data using the up-crossing method was used to find other parameters such as wave length and the slope parameter S at breaking.

Here we compare the experimental data with the similar results for H/h obtained for regular waves by Svendsen & Hansen (1976). They found that, in experiments with regular waves, H/h at breaking is very well predicted by the local value of the slope parameter

$$S = h_x \frac{L}{h} \tag{3}$$

where h_x is the bottom slope. Svendsen (1987) suggested the following empirical formula as fit to the aforementioned experiments:

$$\left(\frac{H}{h}\right)_b = 1.9 \left(\frac{S_b}{1 - 2S_b}\right)^{\frac{1}{2}} \tag{4}$$

where S_b is the value of S at the breaking point. Hansen (1990) gives a simpler approximation to the data for the range $0.25 < S < 1$ as

$$\left(\frac{H}{h}\right)_b = 1.05 S^{0.20} \tag{5}$$

Figure 4 shows results for the $(H/h)_b$ values for each of the four experiments W01, W03, W06, and W07 separately along with the variation according to (4) and (5).

We see that in experiment W01, with only $\pm 10\%$ wave height modulation, the wave breaking quite closely follows the predictions for monochromatic waves. From Table 2 we also see that the order in which these waves break follows their initial heights: wave 3 first, then 4 and 2, and finally 1 and 5. The height of the waves is reversed, however: wave 3 has the smallest breaker height ($(H/h)_b = 0.93$), 1 and 5 the largest (1.01 and 1.02). Though the differences naturally are small they are significant: immediately after all waves have started to break, the groupiness has been reversed.

In experiment W03 with $\pm 20\%$ groupiness the variation of the breaker heights as a function of S begin to deviate from the results for regular waves and in experiments W06 and W07, with the strong wave height variation ($\pm 50\%$ groupiness) the difference from regular waves is quite significant. In all the three experiments W03, W06 and W07, the deviations from the regular wave breaking criterion show the same characteristics: the wave that reaches the highest $(H/h)_b$ value before breaking is wave no 2 in the group and it has a value of $(H/h)_b$ which is close to the values obtained for regular waves, whereas all other waves in the groups break at smaller values of $(H/h)_b$ (with the exception of wave no 3 in W07), and particularly wave 4 and 5 have very small breaker heights, indeed $(H/h)_b = 0.67 - 0.86$. Furthermore, we see from Table 2 that the waves that break at the largest depth ("first") are waves no 3 and 4 in the group, closely followed by No 5, whereas waves 1 and 2 break noticably later.

Note that, in figure 4, the local wavelength used to calculate S_b has been determined from the actual period of the particular wave in the group as measured from the time series. For waves 4 and 5 in experiments W06 and W07 the shift in wave periods illustrated in figure 3 leads to smaller wave lengths and hence smaller S_b - values. The smaller H/h-values at breaking for those waves may be caused by the increase in steepness associated with the change in wave length. Their $(H/h)_b$-values are still much smaller than for regular waves with the same L/h-ratio, though.

It should be remembered that the short waves feel the orbital velocity of the long waves almost as a time varying current, which part of the time is onshore and part of the time offshore. This changes the absolute speed of each wave and, consequently, the wave steepness. The mechanism is complicated, however, because the relative phase between the (propagating) short wave groups and the (partly standing) infragravity wave changes from point to point and the effect requires some distance to accumulate. This issue will be analysed more closely in a second paper.

6.2 Wave Groupiness in the surf-zone.

A second important question is how the groupiness of the short waves is transmitted into the surfzone. List (1991) used field data to analyze this phenomena and found that wave breaking significantly alters the groupiness of the waves. The groupiness was seen to decrease as the shoreline was approached.

Clearly the key to the amount of modulation inside the surf-zone is the effect of groupiness on the breaker height and position described above. But the effect is complicated by the fact that a wave that breaks early with perhaps a large $(H/h)_b$-value also starts decaying early and hence as it reaches the position where one of the other waves break - maybe with a smaller $(H/h)_b$-value - its height may have decreased below the height of that wave.

The wave height variation of the different waves in the group are shown for each experiment in figures 5 and 6.

For W01 in figure 5, which had groupiness of only $\pm 10\%$, it appears that the small variation observed in breaker height and position causes a change in the relative height of the waves after breaking which corresponds to a reversal of the groupiness. In the outer part of the surf-zone this can be identified from figure 5 where waves no 1 and 5 are larger than the other waves and wave no 3 is the smallest. Essentially this also means a phase shift in the group position which obviously changes the forcing on the shoreward propagating, already generated long wave component. Further into the surf-zone this effect is evened out, however, and close to the shoreline the groupiness was actually very small. However, a close inspection of the data shows that the groupiness stays reversed in the entire surf-zone.

For W03, with a groupiness of $\pm 20\%$, a different trend was noticed. As figure 5 shows the highest wave (wave 3) has become smaller than the the two waves in front (wave 1 and wave 2) at the time those two waves start breaking, but stays higher than the two waves behind (wave 4 and wave 5). The pattern observed was that the increased groupiness widens the breaking region so that the wave which breaks early loses energy for a considerably longer distance before it reaches the point where the last wave starts breaking. This means that a partial reversal of groupiness occurs for this case: into the surf-zone the largest waves are waves 1 and 2 and the waves are, in order of decreasing wave height 2, 1, 3, 5 and 4, so that the top of the wave groups has shifted from wave 3 to between waves 1 and 2. The partially reversed groupiness was sustained to a considerable degree almost all the way to the shoreline. Thus because of the difference in breaker position the ordering of the waves according to height at breaking is not necessarily the same as the ordering inside the surf-zone.

In W06 and W07, with a groupiness of $\pm 50\%$ (figure 6), a partial reversal of groupiness is again observed. After breaking the highest wave is wave no 2 closely followed by wave no 1 whereas waves 3, 4, and 5 are progressively smaller. As figure 7 shows, however, these changes are also accompanied by noticeable changes in the periods (hence the lengths) of the waves: the periods of wave 2 and 3 increase considerably at the expense of the period of waves 4 and 5. This is again consistent with the idea that the higher waves poropagate faster than the smaller waves. In both these cases it turns out that far into the surf-zone wave no 5 overtakes the wave no 4 in front of it. The details of this event is shown in figure 8.

It is important to realize that these changes affect the phases of the variations of the radiation stress which is responsible for the long wave generation that continues into the surf-zone.

6.3 Analysis of the spectra.

Some information about the wave motion can be obtained from the wave spectra. The spectral characteristics of the generated waves are shown in figure 9 which gives the powerspectrum versus the frequency (normalized by the short wave frequency f_p) at the reference gage at $x = 4.6\,m$ for W01, W03, and $x = 4.0\,m$ for W06 and W07. We see that, for all experiments, the peak frequency was at the short wave frequency. Since the waves are generated as cnoidal waves substantial amounts of energy is distributed to the subharmonic frequencies from the beginning. The measurements were taken after so long time that all initial disturbances at the eigenfrequencies of the tank had died out. Hence, the longwave motion in the tank is at the period of the groupiness and the sum and difference interactions with the short wave motion.

Since infragravity wave component is not included in the wavemaker signal, all longwave motion in the flume is generated by non-linear interactions: as the short wave motion propagates down the tank it generates a (forced) long wave that propagates with the wave groups. Inside the surf-zone the short wave energy is dissipated and the incoming long wave wave is reflected from the shore. Propagating back out to the wavemaker, this wave is again reflected because we do not absorb the "out-going" long wave motion at the wavemaker. Consequently, the total long wave motion in the tank consists of the first approximation of a shoreward propagating forced wave that is generated over distance from the wavemaker and continuously modified till it reaches the shoreline, and a standing long wave. This corresponds to the peak in the spectra at the relative group frequency of $f_p/5$.

As the waves propagate down the flume, however, energy is also transferred to the neighboring frequencies, due to nonlinear interactions. We see that for W01 the spectrum at the reference gage mainly consists of the short wave peak and its higher harmonics plus a peak at the group frequency. Only weak components at the sum and difference frequencies for the short wave and the group frequencies are observed.

In contrast, the spectra for the three experiments W03, W06 and W07, all show a large number of well defined peaks. While the highest amount of energy is still at the short wave frequency, the modulation of the short waves is much stronger than for experiment W01 (20% and 50% respectively), which means that energy is substantial at the sum and difference frequencies as both first and higher harmonics interact with the group frequency. Since the ratio between the frequencies of the short and long wave components in the original signal is 5:1, all nonlinear interactions result in peaks at frequencies that are multiples of the group frequency.

Similarly, figure 10 shows the energy distribution at various locations on the slope for experiment W03. For reference, the distribution at the toe of the beach is reproduced at the top left. The top right ($x = 18.30\,m$) is a location in the shoaling region. The figures at the bottom ($x = 21.30\,m$ and $x = 23.80\,m$) are in the surf-zone. The growth of the higher harmonics as the waves propagate shoreward is clearly seen. Inside the surf-zone, the energy is even more uniformly distributed at all frequencies that are integer multiples of the group frequency.

6.4 Analysis of the long wave motion.

The existence of long wave motion in the tank is indicated by the presence of energy at frequencies lower than the peak frequency. The spectra of the wave field shows that the energy due to the long wave motion is predominantly at the group frequency. To study the long wave amplitude variation across the wave tank separately, the gage data was low-pass filtered with the upper cut-off at half the peak frequency. A Fourier decomposition method was used to determine the amplitudes of the standing long waves and that of the propagating long waves in the tank.

Since the wavemaker only generates the amplitude modulated short wave motion, the set-down wave associated with the wave groups is produced by the waves as they propagate down the tank, taking the energy out of the short wave motion. Sufficiently far from the wave maker, the equilibrium amplitude of the incoming forced wave would be given by the equilibrium (bound wave) value

$$\bar{\xi}(x,t) = \frac{\partial S_{xx} x}{\rho g H^2} \tag{6}$$

where S_{xx} is the radiation stress in the short wave motion. No attempt has been made, however, to verify whether this equilibrium value was actually reached before the wave reaches the toe of

the slope. This is the reason why we consistently have used the term "forced wave" rather than "bound wave". Another reason is that, on the slope, the transformation of the short waves, both before and after breaking, represent a change in the long wave forcing. This means the long wave motion becomes a combination of free and the equilibrium bound motion which changes continuously towards the shoreline.

At the shoreline of a slope as gentle as 1:35.05 in the experiments, the short wave height approaches zero. This means that before the short waves reach the shore they become so small that breaking ceases. In the laboratory capillary effects can be seen to take over. It is also very clear from watching the long period motion of the shoreline that, apart from viscous effects, that the long wave motion is fully reflected from the shore.

Thus the long wave energy that reaches the shore is essentially sent back out as a free long wave which eventually is re-reflected from the wavemaker, and over time this process creates the standing component of the long wave motion. The consequence of this is that the total long wave motion in the tank can be expected to consist of a propagating forced long wave that represents the combined free and bound long wave components (with the group frequency) that is generated by the short waves on their way to the shore, plus a standing (free) long wave system (again with the group frequency) which is the result of the long wave motion reflected from the shore and re-reflected from the wavemaker (Note that on a real coast, where there is no reflecting wave maker, the standing wave system is replaced by just an outgoing long wave.).

This was utilized in the analysis of the long wave motion by assuming that at each gage the long wave motion in the tank can be represented by an expression of two such components

$$\eta_l(x_j,t) = a(x_j)e^{i(kx_j-\omega t)} + bJ_0\left(\frac{2\omega}{\sqrt{gh}}(l-x_j)\right)e^{-i\omega t} \tag{7}$$

where a and b are the amplitudes of the different components. This expression assumes that the long wave motion in the flume can be adequately described by linear theory. Notice that $a = a(x)$ and that the x variation of a includes the shoaling coefficient in addition to the variation caused by the short wave forcing. Notice also that due to the phase shifts in the groupiness of the short waves and differences in propagation speeds of the short breaking waves and long waves, this forcing can theoretically reduce the amplitude of the long wave.

The result of the assumption that the long wave motion in the tank can be represented by (7) is that the total energy of the long wave in the tank, $\sum_x \eta_l^2(x,t)$, where the summation is over all x locations, is periodic in time. The minimum of $\sum_x \eta_l^2(x,t)$ occurs when the instantaneous water surface elevation due to the standing wave is zero. This then implies that at that time, t_0, the long wave surface elevation in the tank is entirely due to the propagating long wave. Therefore, the variation of $\eta_l(x)$ at $t = t_0$ is used to obtain the amplitude and phase of the propagating long wave. This also implies that at time $t = t_0 + T_g/4$, the standing wave energy has reached its maximum. Consequently, introducing a phase shift of $T_g/4$ in the mathematical expression for the propagating long wave and subtracting that motion from the total long wave motion at $t = t_0 + T_g/4$ should give the maximum of the standing long wave. The standing wave amplitude, b, which is a constant in x is then calculated from that motion using a least-square approximation (Note that the maximum of $\sum_x \eta_l^2(x,t)$, which depends on the amplitude and phase differences between the standing wave and the propagating wave, need not necessarily occur at this time). Furthermore, the envelope and the phase of the propagating long wave can be obtained if we at $t = t_0$ calculate the Hilbert Transform in x of $\eta_l(x,t_0)$, at each x-location. This envelope represents the variation of $a(x)$ along the tank.

This procedure turns out to be quite successful in determining the long wave motion. The results of the analysis for experiments W01, W03, W06 and W07 are presented in figures 11 - 14. In these figures, part (a) shows the long wave motion $\eta_l(x, t_0)$, at the time of minimum energy, part (b) shows the amplitude variation at $t = t_0$ of $\eta_l(x, t_0)$ determined from the Hilbert trnasforms, and part (c) shows the data obtained for the standing wave and the analytical result given by (7) using least-squares for b as described above.

It can be seen from figure 11(b) that for experiment W01 the amplitude of the propagating wave increases till around $x = 15\,m$ and then is relatively constant till around $x = 21\,m$. The breaking region for this experiment is between $x = 22.0\,m$ and $x = 22.7\,m$ and there is significant scatter in the results in the region after breaking. The results suggest, however, that the amplitude of the propagating wave decreases rapidly in this region. If this is correct it suggests that in this region the forcing from the short waves is actually counteracting the long wave motion, as mentioned earlier. After about $x = 23\,m$, the propagating wave again shows increasing amplitude.

For W03 (figure 12), the amplitude of the propagating wave does not seem to reach a constant value. On the other hand, in contrast to W01, the propagating wave shows a marked decrease in amplitude even before the wave actually reach the breaking region, which, for this case is between $x = 19.1\,m$ and $x = 20.45\,m$. This amplitude continues to decrease steadily as the waves approach the shoreline. Also the assumed zeroth-order Bessel approximation for the standing wave does not agree too well, near the shoreline, with the surface amplitudes computed from the data by the above procedure.

For W06 (figure 13), decrease in the propagating wave amplitude seems to start even earlier and it decreases till almost the end of the breaking region (the breaking region is between $x = 19.1\,m$ and $x = 21.4\,m$), after which the amplitude increases and attains a constant value. In this case, the standing wave is very well represented by the zeroth-order bessel function, especially in the surf-zone.

In the case of W07 (figure 14), the propagating long wave increases in amplitude as the breaking region is approached (breaking region here is between $x = 19.1\,m$ and $x = 21.8\,m$). The amplitude decreases in the breaking region and then again as the waves approach the shoreline. There are two distinct peaks in the energy of the propagating wave, one around the start of the breaking region and another in the middle of the surf-zone. The standing wave is again seen to be well represented by the zeroth-order bessel function.

From these figures, it is possible to conclude that energy is exchanged between the propagating long wave and the short waves. However, in all of the four cases presented here, there are regions where the amplitude of this long wave decreases after breaking and in one case (W03), the amplitude continuously decreases after reaching a maximum.

The amplitudes of the standing wave component, calculated using the least-squares error method, for each experiment are tabulated in Table 4. When comparing these results it seems surprising that the amplitudes for experiments W06 and W07 are comparable to the amplitudes in experiment W03, in spite of the fact that the groupiness for W03 ($\pm 20\%$) is only half the groupiness ($\pm 50\%$) in experiments W06 and W07, and the general short wave heights are largely the same.

One possible explanation for this would be that some of the forcing frequencies are close to a seiching mode of the tank and hence would be close to generating resonance in the flume. To verify this, the seiching modes in the flume were found analytically, using linear theory.

The equation governing the seiching in the flume is

$$\frac{\partial^2 \eta}{\partial t^2} - \frac{\partial}{\partial x}\left(gh(x)\frac{\partial \eta}{\partial x}\right) = 0 \tag{8}$$

Assuming periodic and sinusoidal variation for η , $\eta(x,t) = \zeta(x)\cos(\omega t)$, we have

$$\frac{\partial}{\partial x}\left(gh(x)\frac{\partial \zeta}{\partial x}\right) + \omega^2 \zeta = 0 \tag{9}$$

For the tank, the bottom is defined by

$$h(x) = \begin{cases} h_0 & x < x_0 \\ \frac{h_0(l-x)}{l-x_0} & x \geq x_0 \end{cases} \tag{10}$$

where x_0 is the toe of the beach. Equation (8) is solved separately for the two regions of differing bottom slopes and the resulting solutions are match at the toe of the beach, i.e. at $x = x_0$. At the wavemaker ($x = 0\,m$), we have an antinode and at the shoreline ($x = 25.85\,m$), the solution is bounded. The corresponding seiche frequencies for the tank are shown in (Table 5).

Comparison with the group periods for each experiment shown in Table 1 shows that in experiment W01, the linear seiching period closest to the group period is the fourth seiching mode, but the two periods are not close enough to the group wave period for resonant interaction to develop. However, experiment W03 has a group period very close to the third seiching mode, which means that the long wave amplitudes along the tank will become quite large. Conversely in experiments W06 and W07, the group periods lie between two seiching modes. We also see from the spectra for W06 and W07 that there is no energy at those two seiching modes. This seems to confirm the suspicion that the relatively large long wave amplitudes in experiment W03 (relative to W06 and W07) are caused by the nearly resonant nature of the long wave generation in experiment W03.

7 Conclusions.

Wave groups incident on a plane beach with slope 1:35 were investigated experimentally. The groups were composed of cnoidal waves with varying heights. Measurements were obtained from a number of locations in the breaking region as well as inside the surf-zone. The results of the analysis can be summarized as follows:

- All non-linear interactions result in energy at frequencies that are integer multiples of the group frequency. This was found to be true even inside the surf-zone, where the waves have a steep front and the high frequency motion is very energetic.
- The location of the start of breaking of the individual waves in a group is affected by the groupiness of the waves. Although the H/h ratio at breaking was seen to have a wider variation for the individual waves in the group than for monochromatic waves, the deviations were smaller for smaller groupiness at the wave maker.
- The groupiness outside the surf-zone affects the groupiness after breaking. In all cases, some groupiness was observed inside the surf-zone. In one case, it was reversed in the sense that the higher waves in the group before breaking became the smallest after and vice versa. In the other cases, 'partial' reversal of groupiness was observed where the highest wave before breaking became smaller than the waves in front, but remained larger than the two waves behind.

- The long wave motion is forced at the group frequency and can be resolved into two components, an incident forced wave and a standing (free) wave. The standing wave is the result of the reflection of long waves at the wavemaker, where there was no absorption of waves. The amplitude of the incident forced wave varies along the tank, whereas the standing wave is shown largely to agree with a linear representation of a free standing wave system. This seems to confirm the hypothesis that in the nearshore region with a natural coast, the incoming short waves generate long waves even as they are dissipated by breaking. The long waves are fully reflected from the shoreline and propagate back out to sea as free waves that only interact very weakly with the incoming short and long wave motion. In some cases, the group frequency was very close to the seiching mode calculated using linear theory. This gave rise to large amplitudes for the standing wave system in the tank.

Acknowledgements

This work was sponsored by the US Army Reasearch Office, University Research Initiative under contract No. DAAL 03-92-G-0016. The United States government is authorized to produce and distribute reprints for government purposes notwithstanding any copyright notation that may appear herein.

Appendix I: References

Goring, D.G., 1978. Tsunamis-The propagation of long waves onto a shelf. *Rep. No. KH-R-38, W.M.Keck Lab. of Hydraulics and Water Res., CalTech*, Pasadena, California.

Hansen, J.B., 1990. Periodic waves in the surf zone : Analysis of experimental data. *Coastal Engineering, Vol 14*, pp. 19-41.

Kostense, J.K., 1984. Measurements of surf beat and set-down beneath wave groups. *Proceedings of the 19th International Conference on Coastal Engineering*, pp. 724-740.

Longuet-Higgins, M.S. and Stewart, R.W., 1962. Radiation stress and mass transport in gravity waves, with application to surf beats. *Journal of Fluid Mechanics, Vol. 13*, pp. 481-504.

List, J.H., 1991. Wave groupiness variations in the nearshore. *Coastal Engineering, Vol. 15*, pp. 475-496.

Schäffer, H.A., 1990. Infragravity water waves induced by short-wave groups. *Series paper # 50, Institute of Hydrodynamics and Hydraulic Engineering*, Technical University of Denmark.

Schäffer, H.A. and Svendsen, I.A., 1988. Surf beat generation on a mild slope beach. *Proceedings of the 21st International Conference on Coastal Engineering*, pp. 1058-1072.

Southgate, H.N., 1993. Review of wave breaking in shallow water. *HR published paper No. 71, Society of Underwater Technology conference on Wave Kinematics and Environmental forces*, London.

Svendsen, I.A., 1987. Analysis of surf zone turbulence. *Journal of Geophysical research, Vol. 92.*, pp. 5115-5124.

Svendsen, I.A. and Hansen, J.B. 1976. Deformation up to breaking of periodic waves on a beach. *Proceedings of the 15th International Conference on Coastal Engineering*, pp. 477-496.

Symonds, G. Huntley, D.A. and Bowen, A.J., 1982. Two-dimensional surf beat: long wave generation by time varying break point. *Journal of Geophysical Research, Vol. 87*, pp. 492-498.

Watson, G., Barnes, T.C.D. and Peregrine, D.H., 1994. The generation of low-frequency waves by a single wave group incident on a beach. *Proceedings of the 24th International Conference on Coastal Engineering*, pp. 776-790.

Appendix II: Notation

η	-	Water surface elevation
η_l	-	Water surface elevation due to long wave motion
$\bar{\xi}$	-	Equilibrium amplitude of bound long wave
ρ	-	Water density
ω	-	Angular frequency
a	-	Amplitude of propagating component of long wave
b	-	Amplitude of the standing long wave
f_g	-	Group frequency
f_p	-	Peak frequency
g	-	Acceleratin due to gravity
h	-	Water depth calculated assuming slope of 1:35.05
h_0	-	Water depth in the constant depth section of wave tank
h_1	-	Measured water depth
h_x	-	Beach slope
k	-	Wavenumber
l	-	Distance between toe of beach and SWL
G	-	Groupiness factor
H	-	Wave height
H_i	-	Wave height of the i^{th} short wave in the group
H_m	-	Average height of the wave group
ΔH	-	Difference between the maximum and minimum wave height
L	-	Wave length
S	-	Slope parameter
S_b	-	Slope parameter at breaking
S_{xx}	-	Radiation stress
T_g	-	Group period
T_m	-	Period of short waves at wave maker
T_p	-	Peak period
U	-	Ursell Number

Experiment number	H_m/h_0	$T_m\sqrt{g/h_0}$	Peak Frequency (f_p)	Groupiness factor G
W01	0.167	7.43	0.667	$\pm$10%
W02	0.237	12.38	0.4	$\pm$10%
W03	0.237	12.38	0.4	$\pm$20%
W04	0.3	12.38	0.4	$\pm$10%
W05	0.3	12.38	0.4	$\pm$20%
W06	0.25	7.92	0.625	$\pm$50%
W07	0.25	8.67	0.57	$\pm$50%

Table 1: Wave parameters at the wavemaker. H_m is the mean height of the short waves, T_m is the period of the short waves and $h_0(= 0.4\,m)$ is the water depth at the wavemaker.

	W01		W03		W06		W07	
Wave #	$x(m)$	H/h	$x(m)$	H/h	$x(m)$	H/h	$x(m)$	H/h
1	22.60	1.01	20.45	0.95	21.40	0.87	21.80	0.80
2	22.50	0.97	20.15	1.07	21.60	0.98	20.80	0.96
3	22.10	0.93	19.55	0.97	19.20	0.83	19.60	0.95
4	22.30	0.96	19.10	0.86	19.50	0.74	19.40	0.73
5	22.70	1.02	19.65	0.82	19.70	0.69	20.00	0.67

Table 2: Breaking location and the H/h ratio at breaking for each wave. At the wavemaker, the third wave was the highest wave in each group.

W01	W03	W06	W07
4.60	4.60	4.00	4.00
11.85	11.85	11.85	11.85
13.50	12.85	12.95	12.95
14.60	13.75	13.85	13.85
15.60	14.75	14.90	14.90
16.80	15.65	15.10	15.10
17.40	16.50	15.30	15.30
17.90	17.20	15.50	15.50
18.50	18.00	15.70	15.70
19.20	:	16.90	16.90
19.40	Every $0.05m$	17.50	17.50
19.80	(except 19.35	17.70	17.70
20.10	20.05 & 20.70)	17.90	17.90
20.50	:	18.10	18.10
20.80	21.10	:	:
21.20	21.30	Every 0.1 m	Every 0.1 m
21.40	21.70	(except 20.60	(except 20.50)
:	22.00	20.80, 21.00	:
Every 0.1 m	22.40	& 21.20)	24.40
:	22.70	:	:
24.50	23.10	24.40	Every $0.05m$
	23.40	:	:
	23.80	Every $0.05m$	25.35
		:	
		25.35	

Table 3: Gage locations for the different experiments.

Experiment Number	Standing wave amplitude (cm)
W01	0.308
W03	4.418
W06	3.708
W07	4.598

Table 4: The amplitude b (as in (7)), at the shoreline, of the long wave components in the tank.

Seiching mode	Frequency (rad/s)	Period (s)
0	0.2084	30.15
1	0.3345	18.78
2	0.5014	12.53
3	0.6795	9.25
4	0.8140	7.72

Table 5: Seiching frequencies and their corresponding periods in the tank.

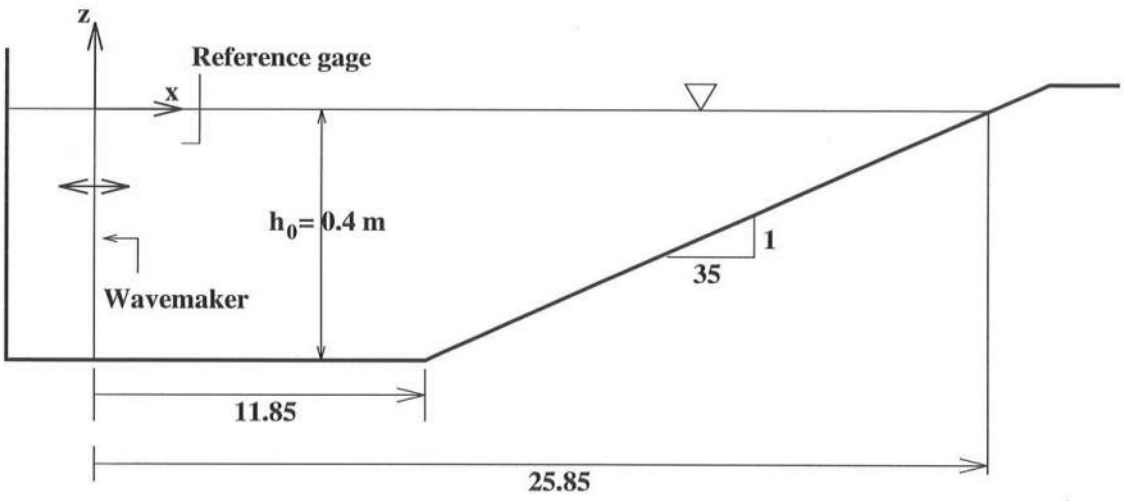

Figure 1: Definition sketch of the experimental setup. The reference gage was at $x = 4.6\ m$ for experiments W01 through W05 and at $x = 4.0\ m$ for experiments W06 & W07.

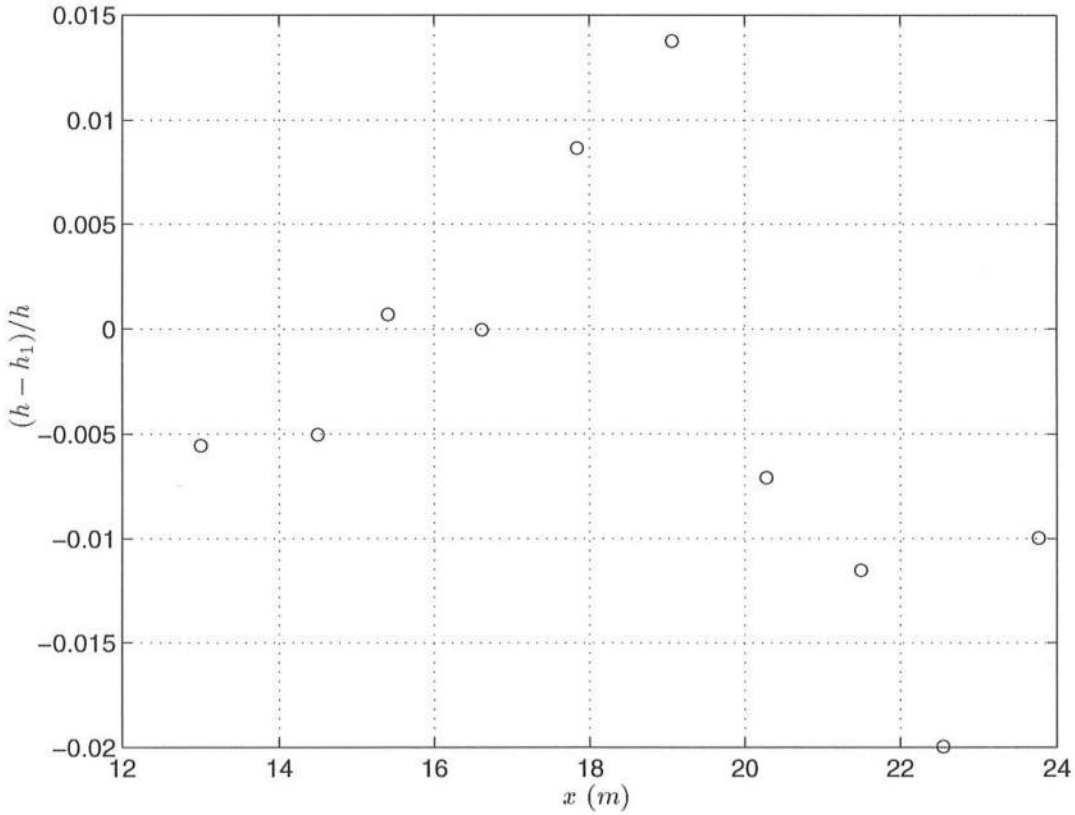

Figure 2: Deviation of the water depth from the average slope calculated according to a least-square fit to the data. h is the calculated local depth and h_1 is the measured depth. The average slope is 1:35.05.

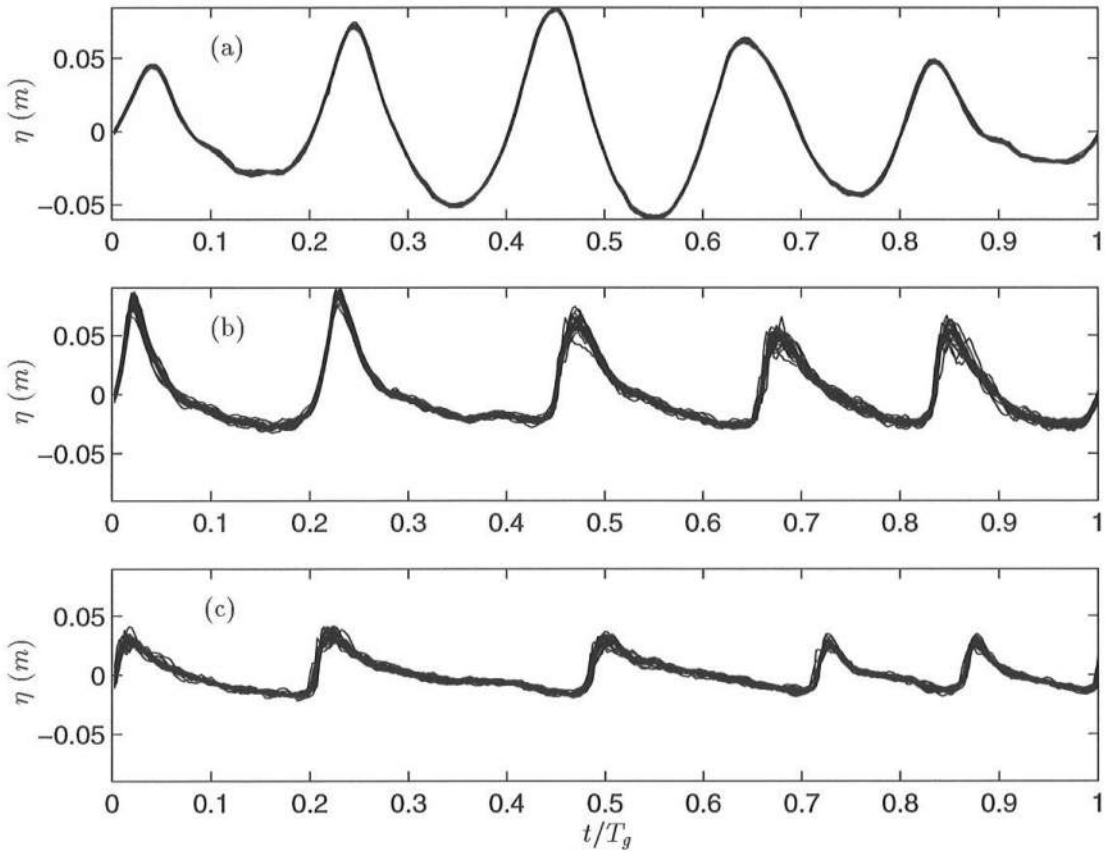

Figure 3: The variability of the wave profiles at three different positions in the tank: (a), at the reference gage, $x = 4.0\ m$, (b), at $x = 20.9\ m$, and (c), at $x = 23.1\ m$, for experiment W06. Breaking occurs between $x = 19.2\ m$ and $x = 21.4\ m$ (see table 2), s, position (b) is around initiation of breaking and (c) is well into the surf-zone.

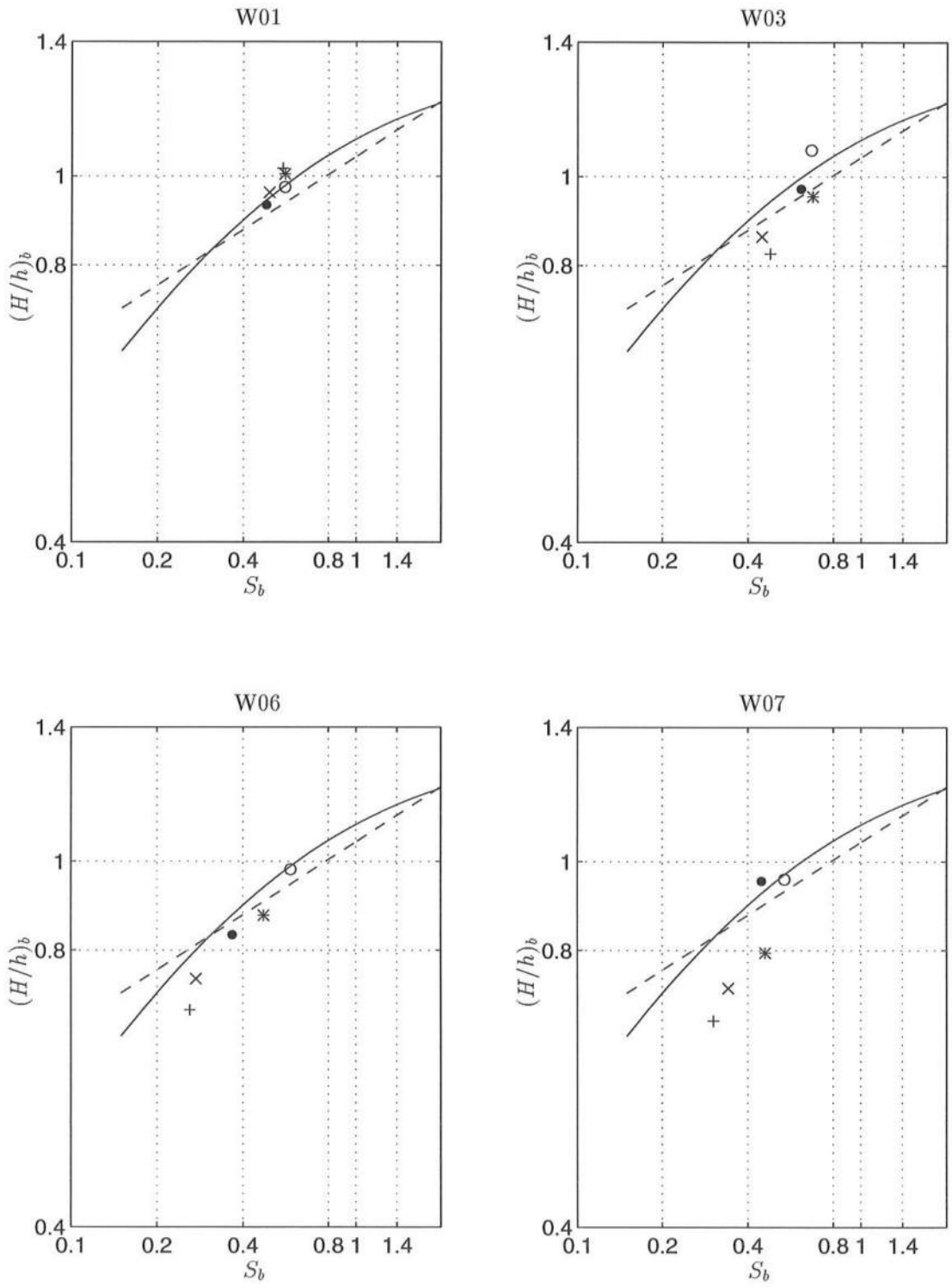

Figure 4: Variation of break point for W01, W03, W06 and W07. The curves shown are from Svendsen, 1987 (———) and Hansen, 1990 (— — —). The points shown are for the individual waves in the group, wave 1 (*), wave 2 (o), wave 3 (•), wave 4 (x) and wave 5 (+).

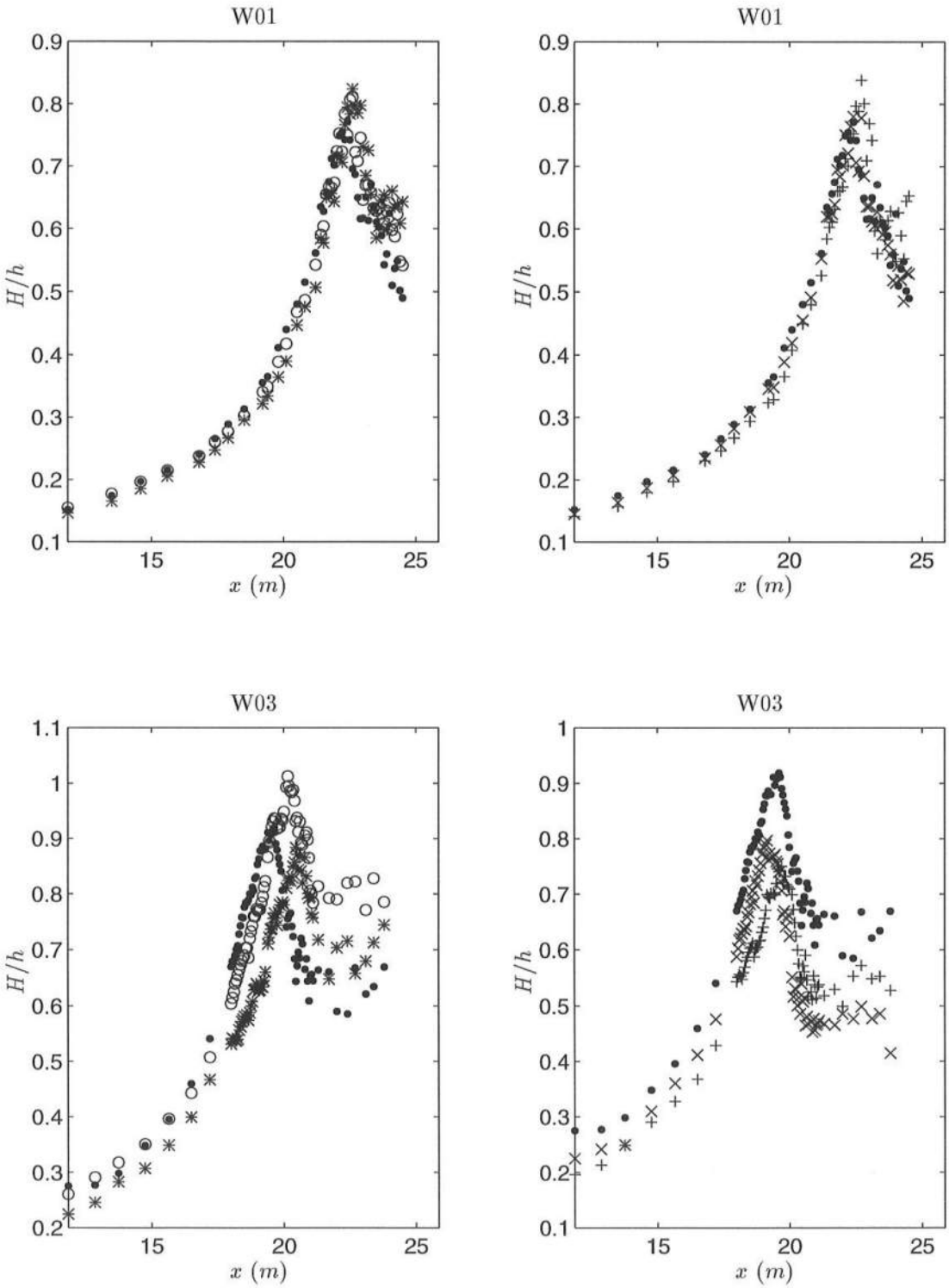

Figure 5: The wave height variation along the tank for wave 1 (*), wave 2 (o), wave 3 (•), wave 4 (x) and wave 5 (+) in the group for W01 and W03. The figures start at the toe of the beach $x = 11.85\,m$ and the data for wave 3 is repeated in the two parts of each figure.

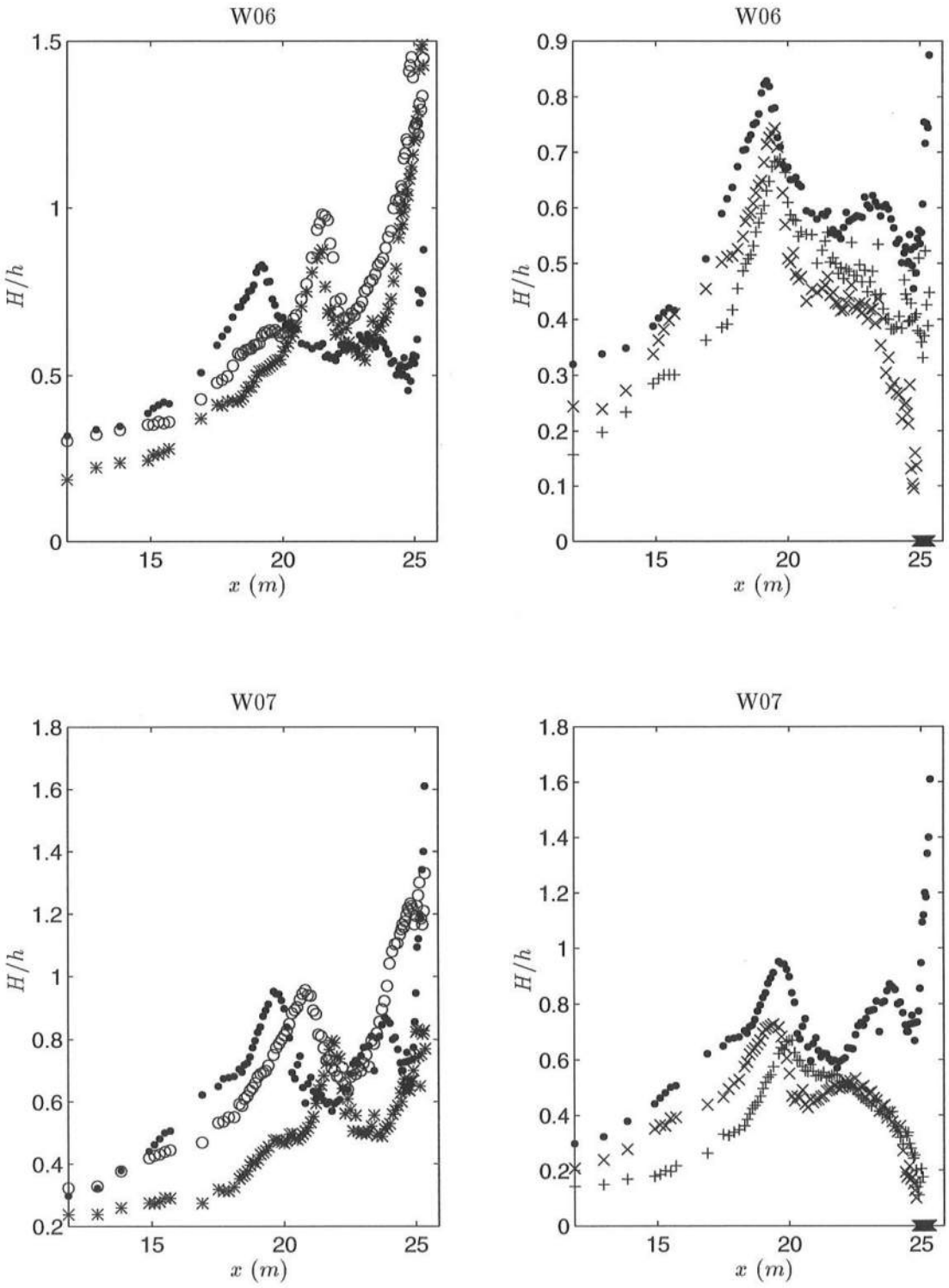

Figure 6: The wave height variation along the tank for wave 1 (*), wave 2 (o), wave 3 (•), wave 4 (x) and wave 5 (+) in the group for W06 and W07. The figures start at the toe of the beach $x = 11.85\,m$ and the data for wave 3 is repeated in the two parts of each figure.

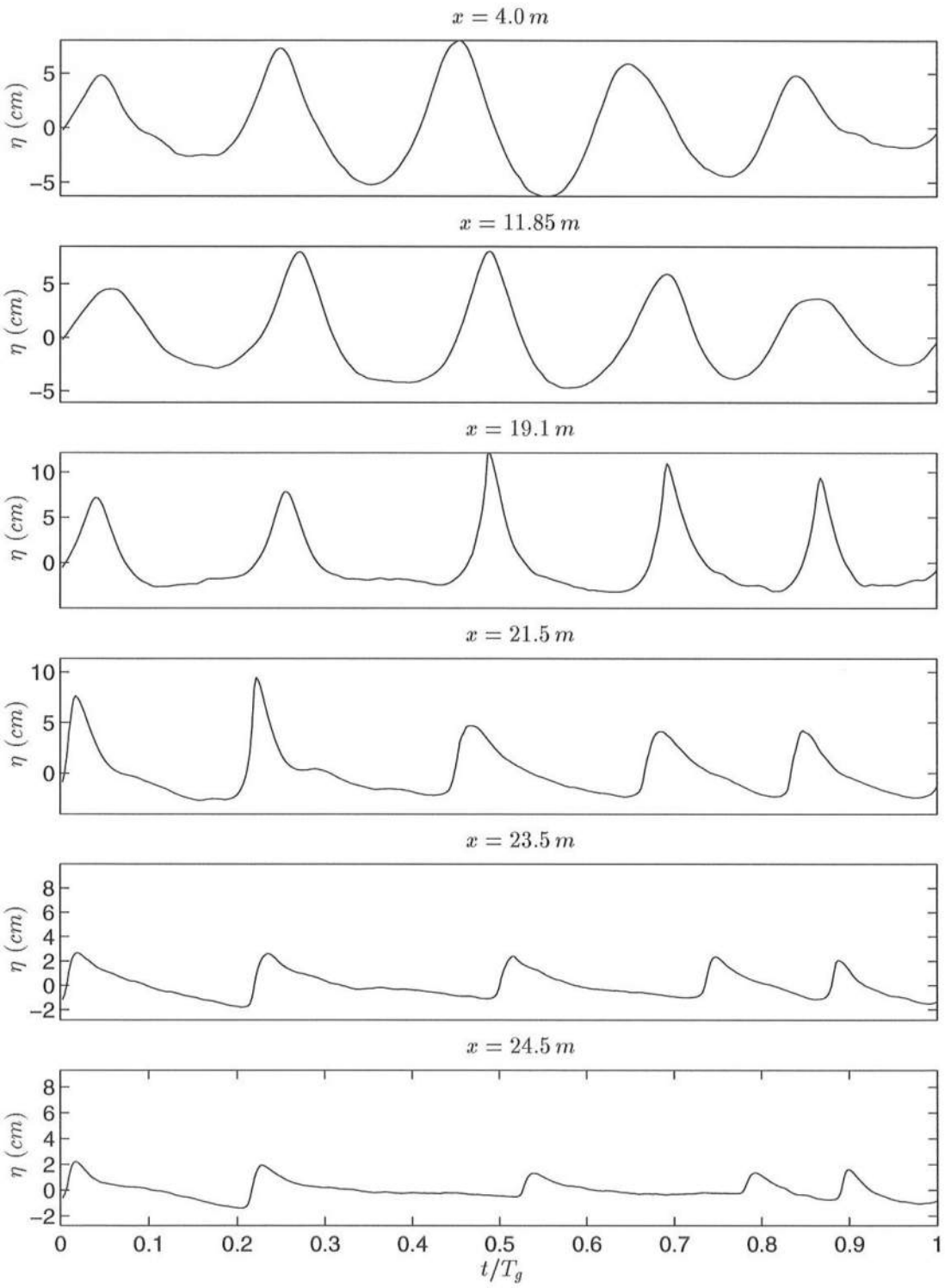

Figure 7: Development of the form of the wave groups for W06 at different locations: $x = 11.85\ m$ is at the toe of the beach, and breaking starts between $x = 19.20\ m$ and $x = 21.60\ m$ (see table 2).

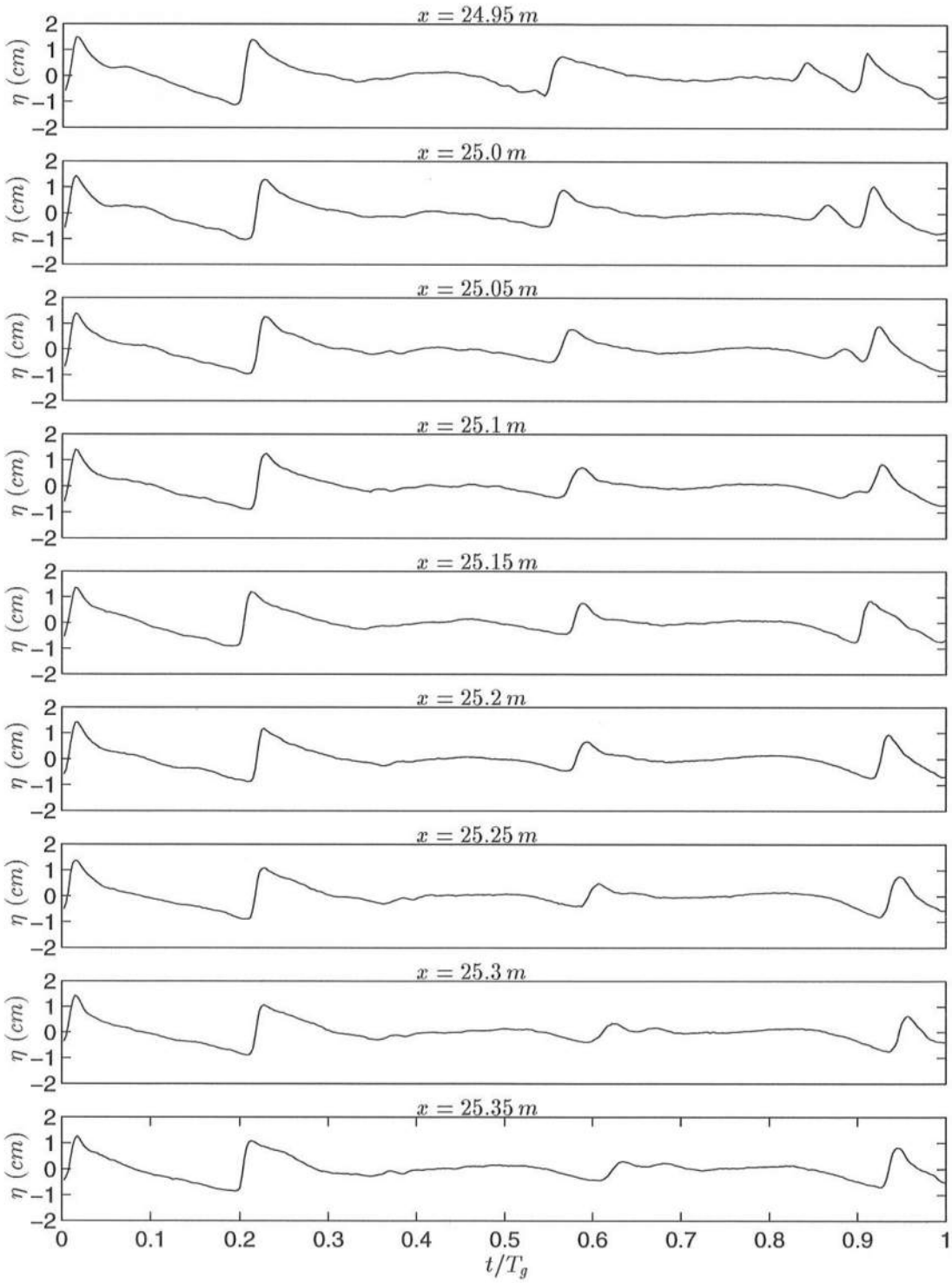

Figure 8: Wave profile development for experiment W06 in the region near the shoreline where wave 4 in the group ceases to exist.

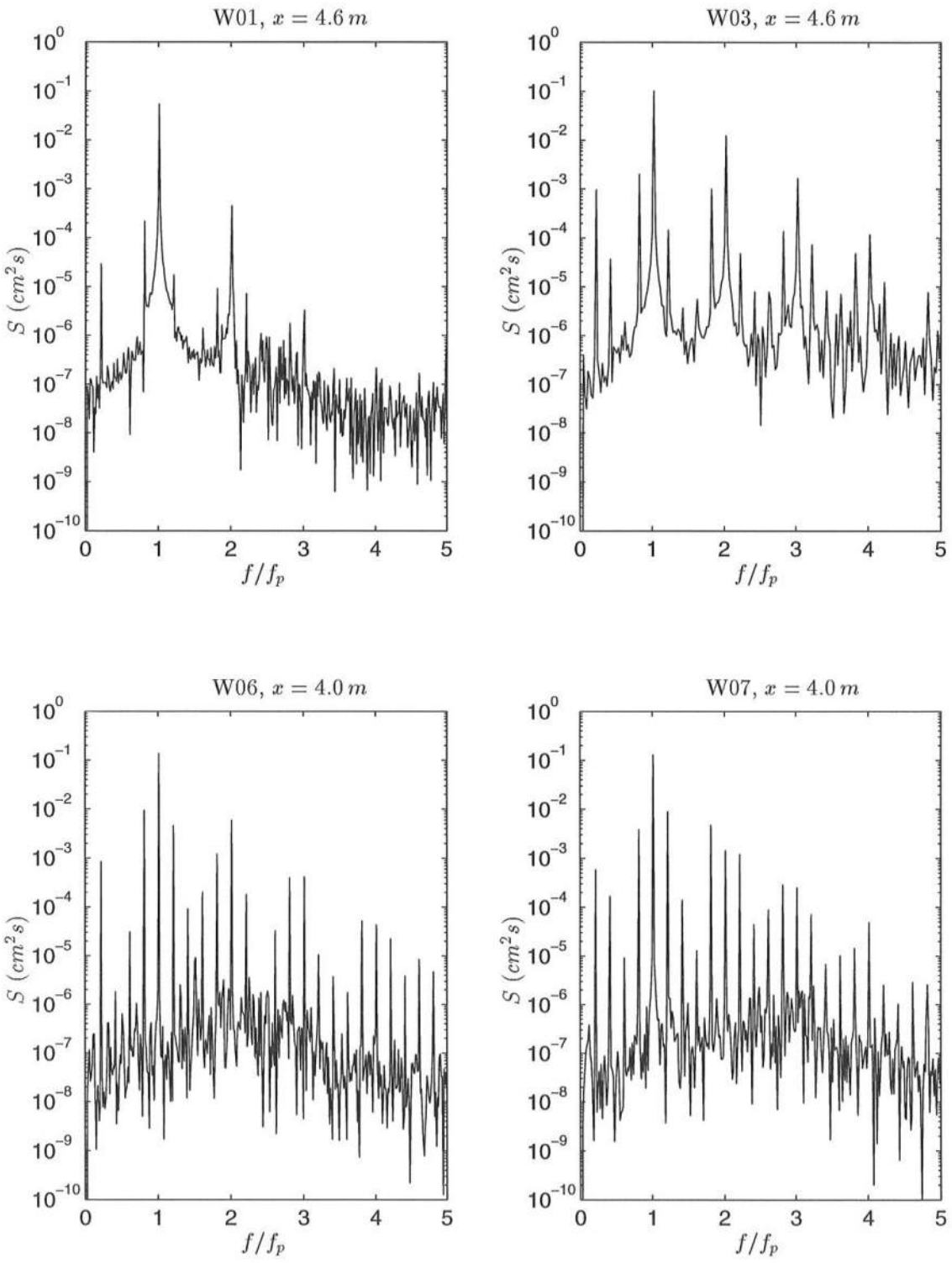

Figure 9: The spectra at the reference gage for experiments W01, W03, W06 and W07. The frequencies have been non-dimentionalized with respect to the short wave frequency (see table 1). Hence, the group frequency f_g is at 0.2.

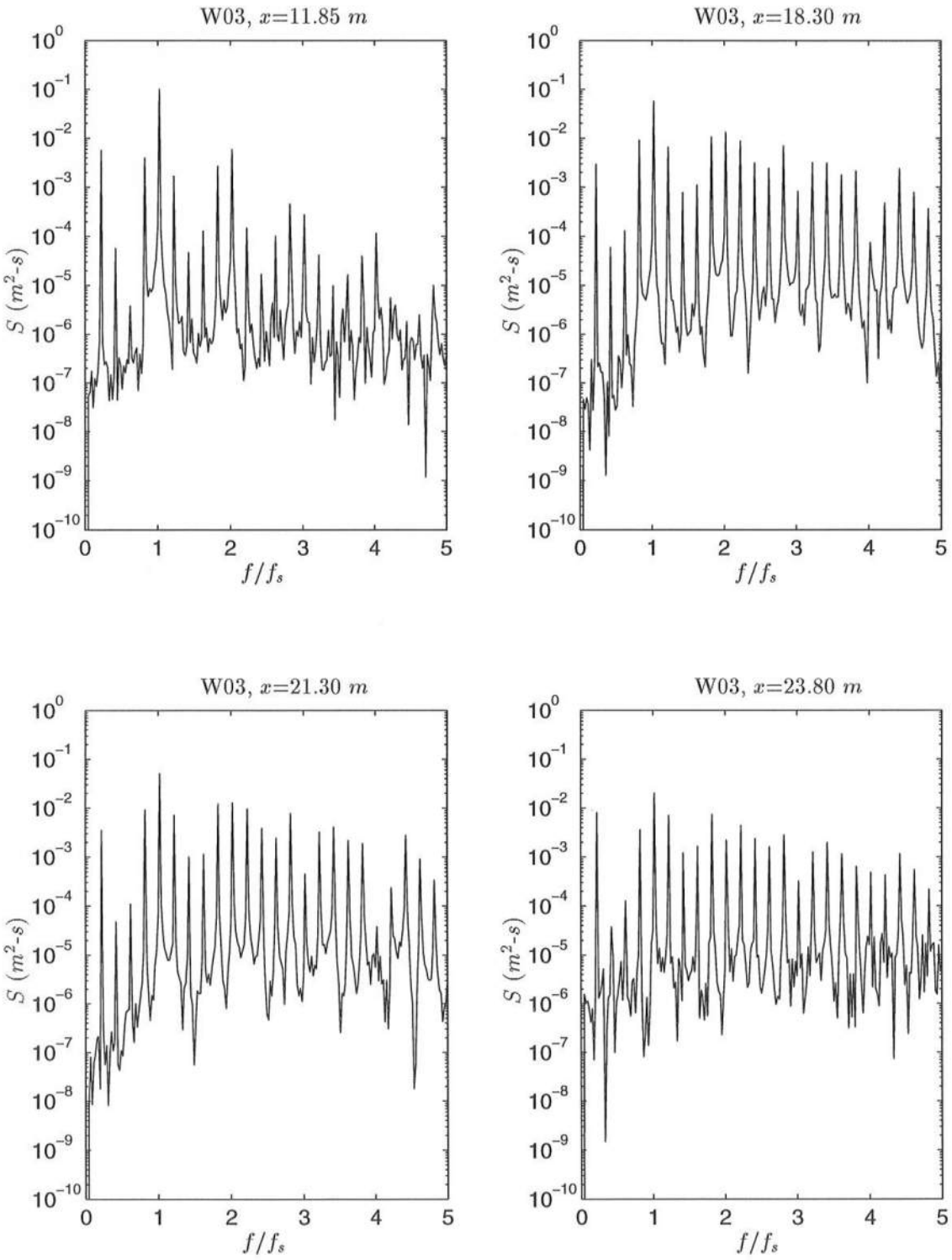

Figure 10: The development of the spectra along the flume for W03. The spectra shows the growth of the energy at the group frequency ($f_g/f_s = 0.2$) relative to the short wave energy, particularly in the surf-zone (between $x = 21.30\ m$ and $x = 23.80\ m$, the last data point in experiment W03).

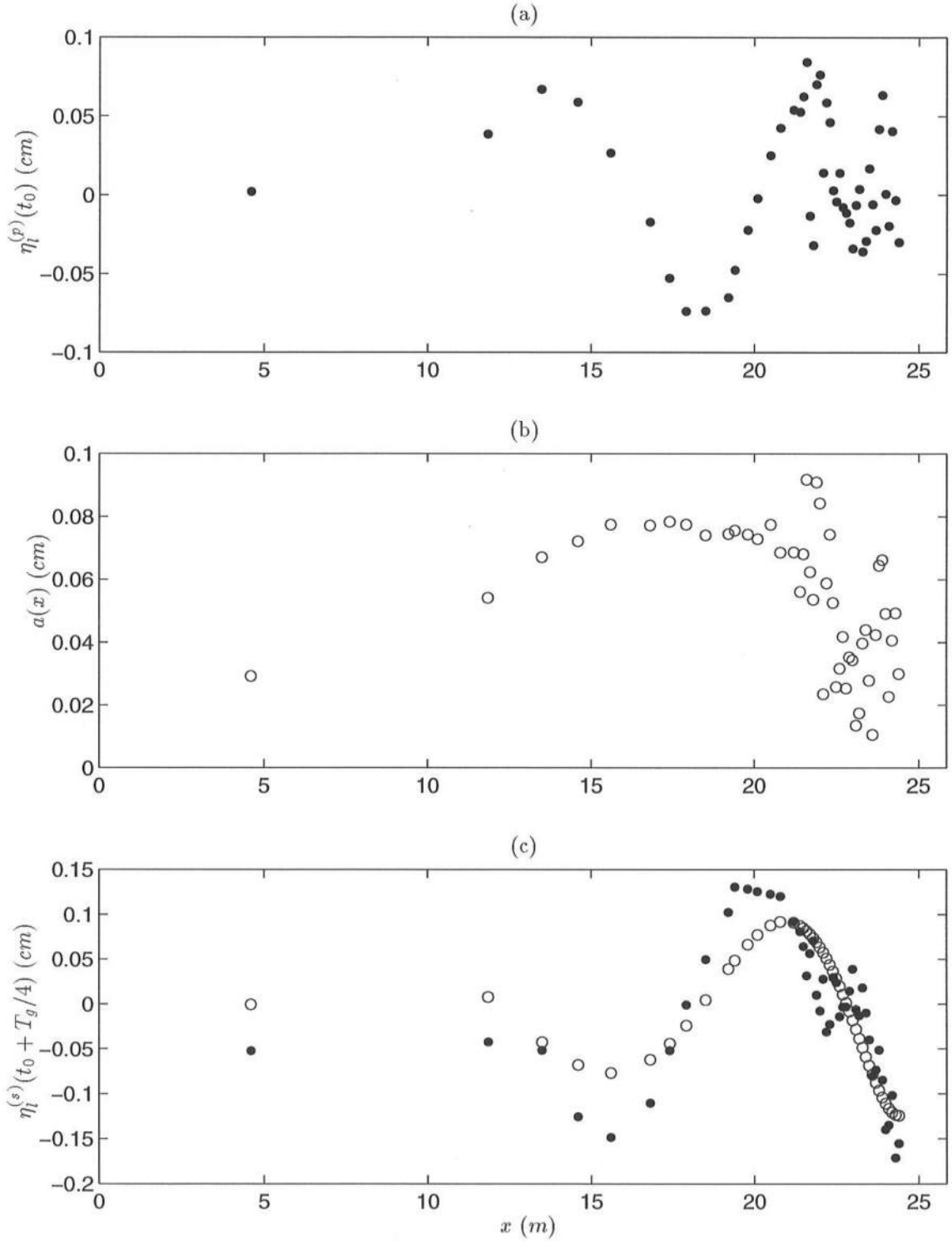

Figure 11: Long wave motion in the tank for W01: (a) water surface elevation of the propagating long wave at time $t = t_0$, (b) amplitude of the propagating long wave as a function of the distance from the wave maker, (c) the standing long wave in the tank at $t = t_0 + T_g/4$ ('•' is data and 'o' is the least-squares fit).

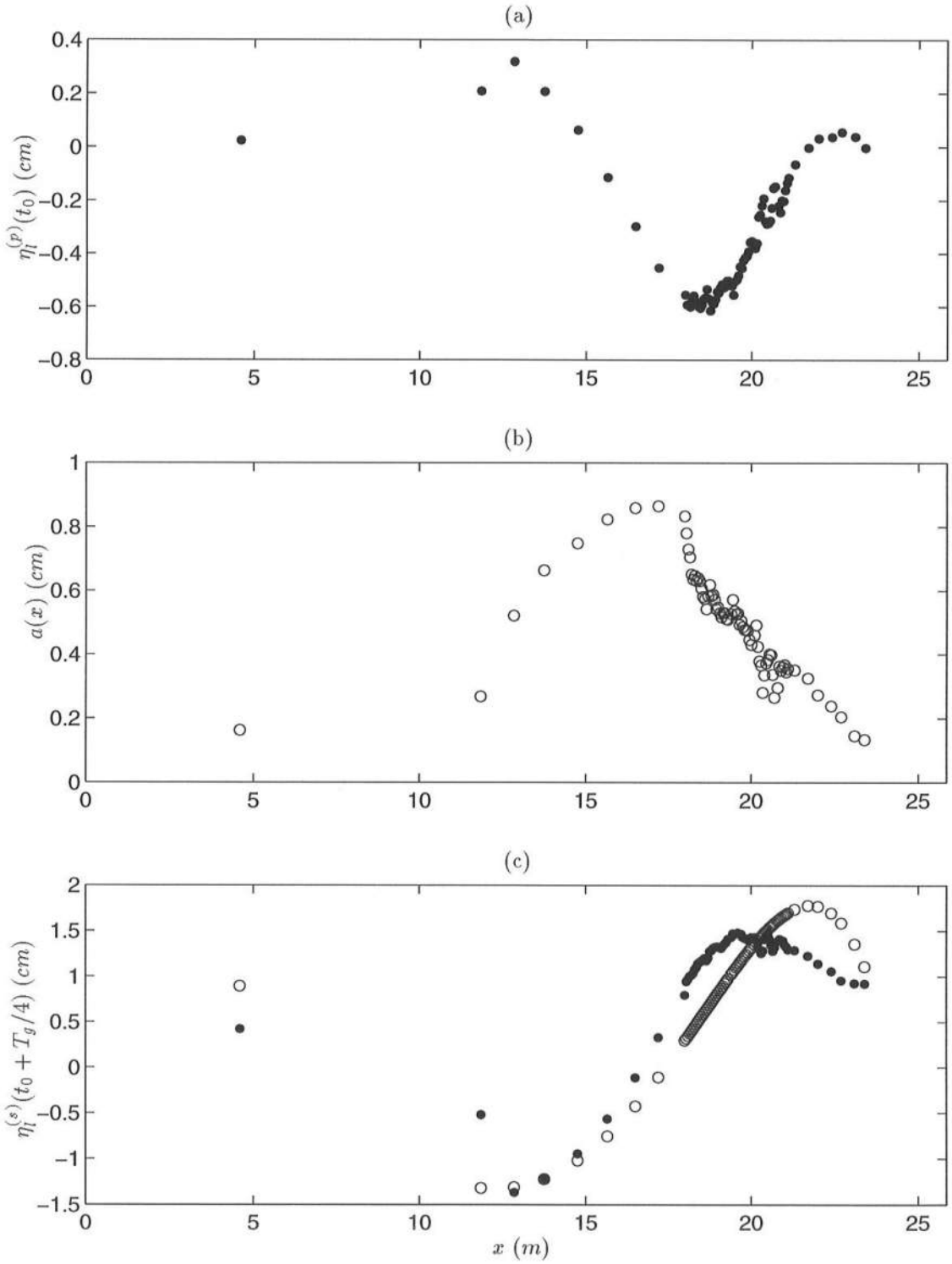

Figure 12: Long wave motion in the tank for W03: (a) water surface elevation of the propagating long wave at time $t = t_0$, (b) amplitude of the propagating long wave as a function of the distance from the wave maker, (c) the standing long wave in the tank at $t = t_0 + T_g/4$ ('•' is data and 'o' is the least-squares fit).

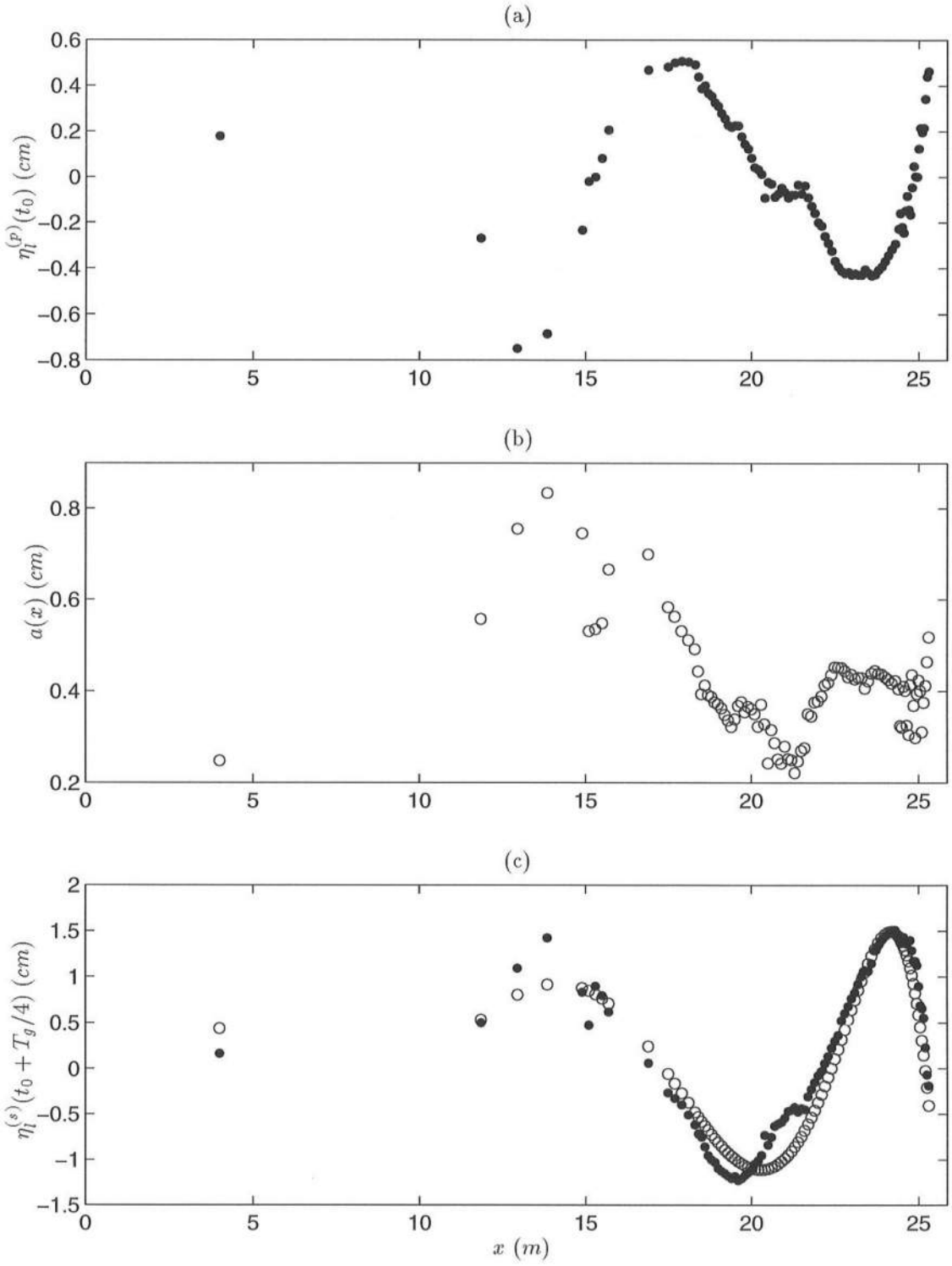

Figure 13: Long wave motion in the tank for W06: (a) water surface elevation of the propagating long wave at time $t = t_0$, (b) amplitude of the propagating long wave as a function of the distance from the wave maker, (c) the standing long wave in the tank at $t = t_0 + T_g/4$ ('•' is data and 'o' is the least-squares fit).

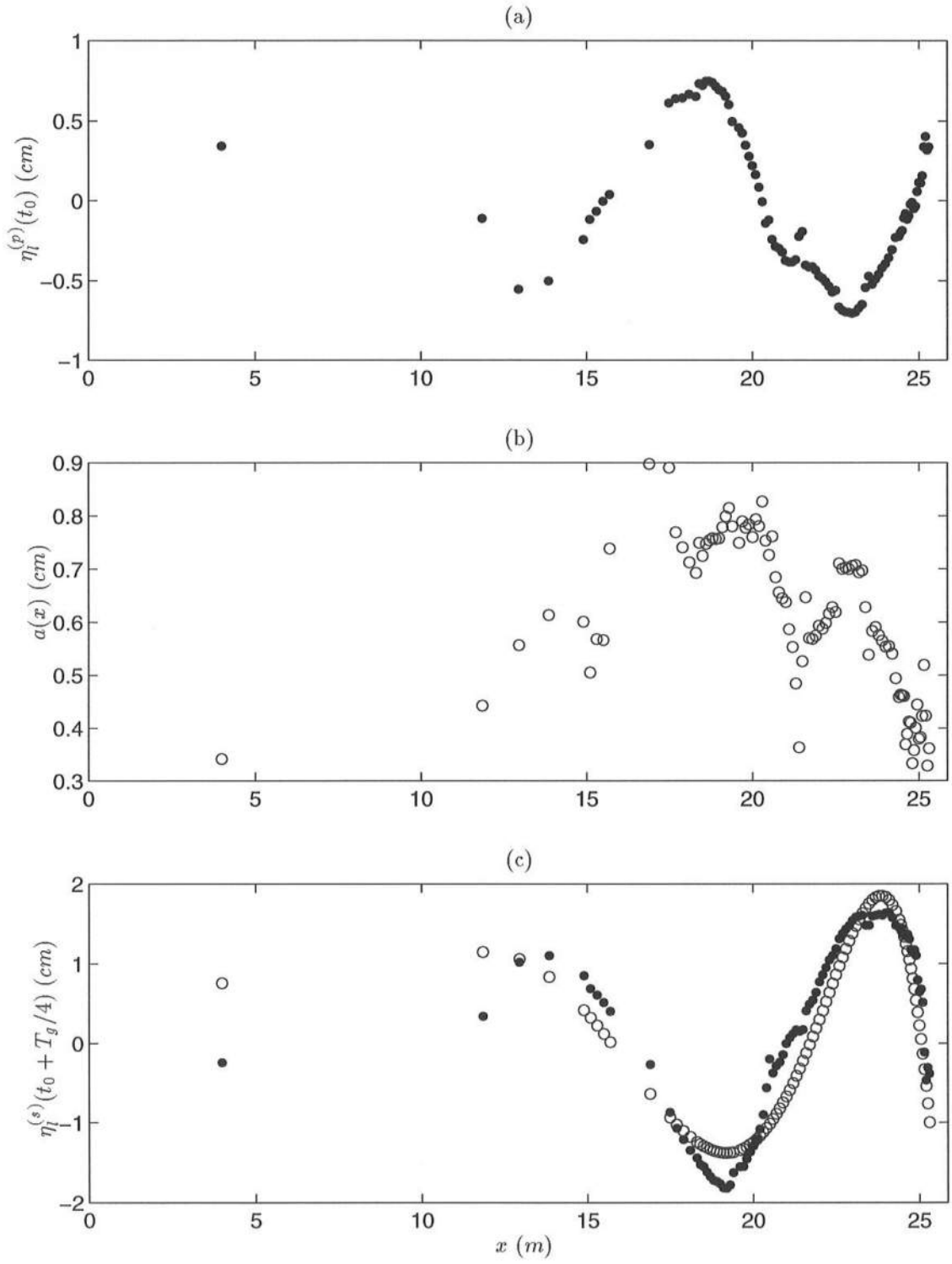

Figure 14: Long wave motion in the tank for W07: (a) water surface elevation of the propagating long wave at time $t = t_0$, (b) amplitude of the propagating long wave as a function of the distance from the wave maker, (c) the standing long wave in the tank at $t = t_0 + T_g/4$ ('•' is data and 'o' is the least-squares fit).